

Matrix product state of multi-time correlations

Katja Klobas¹, Matthieu Vanicat¹, Juan P. Garrahan^{2,3} and
Tomaž Prosen¹

¹ Department of Physics, Faculty of Mathematics and Physics, University of Ljubljana, Ljubljana, Slovenia

² School of Physics and Astronomy, University of Nottingham, Nottingham NG7 2RD, United Kingdom

³ Centre for the Mathematics and Theoretical Physics of Quantum Non-equilibrium Systems, University of Nottingham, Nottingham NG7 2RD, United Kingdom

Abstract. For an interacting spatio-temporal lattice system we introduce a formal way of expressing multi-time correlation functions of local observables located at the same spatial point with a *time state*, a statistical distribution of configurations observed along a time lattice. Such a time state is defined with respect to a particular equilibrium state that is invariant under space and time translations. The concept is developed within the *Rule 54* reversible cellular automaton, for which we explicitly construct a matrix product form of the time state with matrices that act on the 3-dimensional auxiliary space. We use the matrix product state to express equal-space time-dependent density-density correlation function which, for a special maximum-entropy values of equilibrium parameters, agrees with the previous results. Additionally, we obtain an explicit expression for the probabilities of observing all multi-time configurations, which enables us to study distributions of times between consecutive excitations and prove the absence of the decoupling of timescales in the Rule 54 model.

1. Introduction

Computation of time dependent correlation functions of local observables is the central problem when discussing locally interacting models in statistical mechanics, in particular in the studies of non-equilibrium dynamics, transport, thermalization and alike. Multi-time correlation functions in particular are crucial for the understanding of complex dynamics, for example that which occurs in systems displaying metastability such as glass formers (for reviews see e.g. [1–3]). However, obtaining an exact form or at least asymptotic behaviour of such correlation functions is usually out of the scope of the current analytical methods, even for the simplest interacting systems. Sometimes even a partial knowledge of multi-time correlation functions of local observables located at the same point can provide useful insights. For example, when studying the transport of conserved quantities, knowing the multi-time equal-space density-density correlation function provides the scaling behaviour of the central (heat) peak within the hydrodynamic description [4]. On other hand, multi-time equal-space correlation

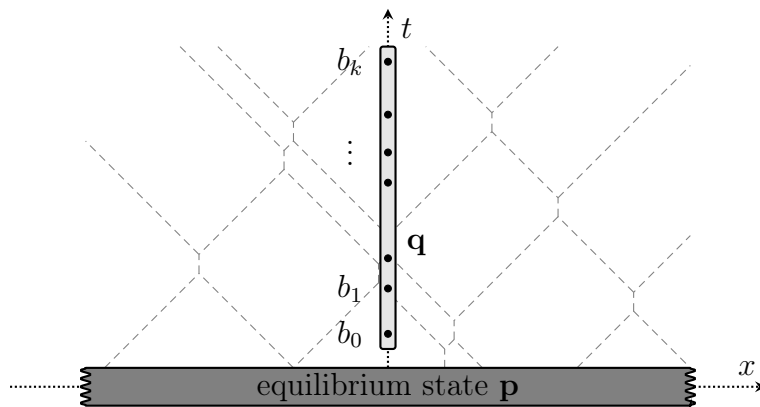


Figure 1. Schematic picture of the setup. We are interested in probability distribution \mathbf{q} of the configurations (b_0, b_1, \dots, b_k) at the center of the chain $x = 0$ and different times t , while the system is in the equilibrium state \mathbf{p} . Intuitively, we can understand this as keeping track of the particles that pass through the origin. Since they are interacting with each other this is generally not a trivial task and the computational complexity of \mathbf{q} might still be growing exponentially with time.

functions can be viewed as expectation values of a specific class of observables that are nonlocal in time but local in space.

Specifically, we will be interested in the multi-point correlation functions of single-site (ultralocal) observables a_j located at the same spatial point $x = 0$ but at different times t_j ,

$$C_{a_1, a_2, \dots, a_k}(t_1, t_2, \dots, t_k) = \langle a_1(0, t_1) a_2(0, t_2) \cdots a_k(0, t_k) \rangle_{\mathbf{p}} \quad (1)$$

where \mathbf{p} denotes an equilibrium state (which is, by definition, time-translation invariant). The computational complexity of time evolution of local observables in interacting systems generically grows exponentially even within classical mechanics ‡, but since all of them are positioned at the same point, one expects that a lot of information contained in the time propagated observables $a_j(x, t)$ is not necessary for knowing the expectation value (1). Therefore we propose that, at least in certain cases, the computational complexity could be reduced by introducing a *time state* $\mathbf{q}(\mathbf{p})$, i.e. the probability distribution of observing *configurations in time* $(b_0, b_1, b_2, \dots, b_k)$ if the system is in the equilibrium state \mathbf{p} , as is schematically shown in Figure 1. Here b_j label a complete set of ultralocal observables.

In the paper we show that it is possible to construct an explicit nontrivial matrix product representation of such states in the case of Rule 54 reversible cellular automaton (RCA54), introduced in [5]. RCA54 is a classical deterministic model in discrete spacetime of particles that move with constant velocities and interact pairwise by shifting for one site when scattering. The model is also closely related to the automaton ERCA 250R as introduced by Takesue [6] and to the Floquet version of Fredrickson-Andersen model [7–9]. The simplicity of the model allows for a lot of exact results to be

‡ By computational complexity we refer to a computational cost of computing the propagated observable exactly, not approximating it.

obtained, such as the non-equilibrium steady state of the system coupled to stochastic reservoirs [10, 11], as well computing the most relevant (long lived) decay modes [12], and exact treatment of large deviation statistics [13]. Furthermore, an explicit matrix product representation of the complete time evolution of local observables was found [14], which was afterwards generalized to time evolution of local density matrices in the quantum version of the model [15].

The paper is structured as follows; in section 2 we define the model and introduce a two-parameter family of equilibrium states. The states are expressed in terms of a matrix product ansatz (MPA) with matrices that obey the cubic cancellation relation introduced in [12]. We express asymptotic probabilities of observing finite subconfigurations in the limit of large system sizes and show that the probabilities of these subconfigurations satisfy a particular factorization property implying statistical independence of solitons. Section 3 contains the main result of the paper, namely an explicit construction of the time state. Due to the statistical independence of solitons, the construction reduces to the problem of keeping track of all the solitons (or quasi-particles, in general) that pass through the site 0. This is achieved by introducing matrices that act on a 3-dimensional auxiliary space and expressing the time state in an MPA form. In sections 4 and 5 we briefly discuss examples of correlation functions and expectation values that can be exactly expressed using the MPA form of the time state. Finally, in section 6 we finish with closing remarks.

2. Rule 54 reversible cellular automaton

2.1. Definition of the dynamics

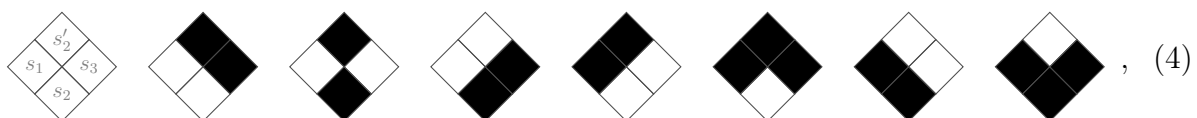
The model is a deterministic cellular automaton defined on a chain of even length $2n$, with every site being either occupied or empty. The configuration of the system at time t is given by the string of bits $(s_1^t, s_2^t, \dots, s_{2n}^t)$, where $s_j^t = 0$ if the site j is empty at time t and $s_j^t = 1$ otherwise. The period-two (staggered) time evolution map consists of two time steps, in the first step only the values on even sites are changed, while in the second step the odd sites are updated

$$s_x^{t+1} = \begin{cases} \chi(s_{x-1}^t, s_x^t, s_{x+1}^t); & x+t \equiv 0 \pmod{2}, \\ s_x^t; & x+t \equiv 1 \pmod{2}, \end{cases} \quad (2)$$

where we assume periodic boundaries, $s_{2n+k}^t \equiv s_k^t$. The local update map χ is given by the *Rule 54* (RCA54) of Bobenko *et. al.* as introduced in [5],

$$\chi(s_1, s_2, s_3) = (s_1 + s_2 + s_3 + s_1 s_3) \pmod{2}. \quad (3)$$

It is convenient to imagine the chain to have a zig-zag shape as schematically shown in Figure 2. Then the local update rule can be expressed graphically by representing occupied sites by black squares and empty sites by white squares,



$$, \quad (4)$$

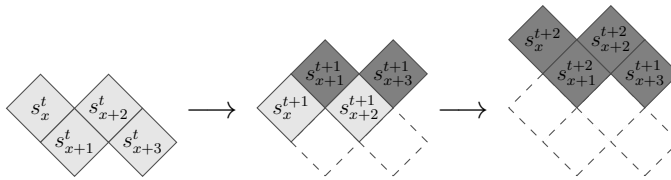


Figure 2. Schematic representation of the lattice geometry and time evolution. Only half of the sites are being updated at the same time (2), therefore it is convenient to imagine the chain to have a zig-zag shape. At each time step, the sites positioned at the bottom (e. g. s_{x+1}^t and s_{x+3}^t on the left most picture) are propagated, while the top sites (s_x^t and s_{x+2}^t) do not change. The new value depends on the values of the three consecutive sites as described in (2) and (4).

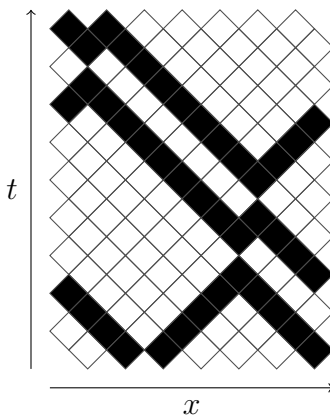


Figure 3. An example of time evolution. We start with a configuration of 14 sites and evolve it according to the rules (4) with periodic boundary conditions. The black sites behave as particles that move with velocity 1 either to the left or to the right. The particles interact *pairwise* by annihilating and then reappearing in the next time step (described by the 3rd, 6th and 8th diagram in (4)). This induces a delay for one site with respect to the original trajectories of the particles.

where bottom three squares represent a configuration of three consecutive sites at time t , (s_1, s_2, s_3) , while the top square is the updated site, $s'_2 = \chi(s_1, s_2, s_3)$. An example of the time evolution induced by these rules is shown in Figure 3.

The graphical representation provides an intuitive interpretation of the dynamics; occupied sites behave as particles that move with velocity ± 1 while undisturbed. When two oppositely moving particles meet, they interact by being delayed for one site (or one time step) with respect to their initial trajectories.

2.2. Time evolution of probability distributions

The states \mathbf{p} are probability distributions over configurations and can be expressed as vectors from $(\mathbb{R}^2)^{\otimes 2n}$ with nonnegative components and the appropriate normalization,

$$\mathbf{p} = (p_0, p_1, \dots, p_{2^{2n}-1}), \quad p_s \geq 0, \quad \sum_{s=0}^{2^{2n}-1} p_s = 1, \quad (5)$$

where p_s is the probability of observing the configuration $(s_1, s_2, \dots, s_{2n})$ given by the binary representation of s ; $s = \sum_{j=1}^{2n} 2^{2n-j} s_j$. The local update rule is given in terms of a three-site permutation matrix P with the elements $P_{(s_1 s_2 s_3), (b_1 b_2 b_3)} = \delta_{s_1, b_1} \delta_{s_2, \chi(b_1, b_2, b_3)} \delta_{s_3, b_3}$. Explicitly,

$$P = \begin{bmatrix} 1 & & & & & \\ & & 1 & & & \\ & & & 1 & & \\ & 1 & & & & \\ & & & & & 1 \\ & & & & & & 1 \\ & & & & 1 & & \\ & & & & & & & 1 \\ & & & & & & & & 1 \end{bmatrix}, \quad P^2 = \mathbb{1}. \quad (6)$$

Introducing the local propagators of triplets of neighbouring sites as $P_{x-1, x, x+1} = \mathbb{1}_{2^{x-2}} \otimes P \otimes \mathbb{1}_{2^{2n-x-1}}$, the time evolution of a state \mathbf{p}^t can be expressed in the following way,

$$\mathbf{p}^{t+1} = \begin{cases} U_e \mathbf{p}^t; & t \equiv 0 \pmod{2}, \\ U_o \mathbf{p}^t; & t \equiv 1 \pmod{2}, \end{cases} \quad (7)$$

$$U_e = \prod_{x=1}^n P_{2x-1, 2x, 2x+1}, \quad U_o = \prod_{x=1}^n P_{2x-2, 2x-1, 2x}.$$

2.3. Equilibrium states

The equilibrium states should be invariant to time evolution for whole periods of time, i.e. for even times t . Since the time propagation is staggered, we can introduce two versions of the equilibrium state, \mathbf{p} and \mathbf{p}' , corresponding to even and odd time steps. In this case the time invariance condition takes the following form,

$$\mathbf{p}' = U_e \mathbf{p}, \quad \mathbf{p} = U_o \mathbf{p}'. \quad (8)$$

In the paper we consider the states that can be expressed in the matrix product form similar to stationary states introduced in [12, 13]. Let $\mathbf{W}(\xi, \omega)$ and $\mathbf{W}'(\xi, \omega)$ be vectors in the physical space,

$$\mathbf{W}(\xi, \omega) = \begin{bmatrix} W_0(\xi, \omega) \\ W_1(\xi, \omega) \end{bmatrix}, \quad \mathbf{W}'(\xi, \omega) = \begin{bmatrix} W'_0(\xi, \omega) \\ W'_1(\xi, \omega) \end{bmatrix}. \quad (9)$$

Their components are 3×3 matrices that depend on two *spectral parameters* ξ and ω ; $\xi, \omega > 0$,

$$W_0(\xi, \omega) = \begin{bmatrix} 1 & 0 & 0 \\ \xi & 0 & 0 \\ 1 & 0 & 0 \end{bmatrix} = W'_0(\omega, \xi), \quad W_1(\xi, \omega) = \begin{bmatrix} 0 & \xi & 0 \\ 0 & 0 & 1 \\ 0 & 0 & \omega \end{bmatrix} = W'_1(\omega, \xi). \quad (10)$$

The two sets of matrices $\mathbf{W}(\xi, \omega)$, $\mathbf{W}'(\xi, \omega)$ are mapped to each other under the exchange of the (spectral) parameters $\xi \leftrightarrow \omega$. In what follows, the explicit dependence

on ξ and ω will sometimes be suppressed to simplify the notation. The matrices obey a cubic algebraic relation

$$P_{123} \mathbf{W}_1 \mathbf{W}'_2 \mathbf{W}_3 S = \mathbf{W}_1 S \mathbf{W}_2 \mathbf{W}'_3, \quad (11)$$

where S is a 3×3 matrix acting on the auxiliary space,

$$S = \begin{bmatrix} 1 & & \\ & 1 & \\ & & 1 \end{bmatrix}, \quad S^2 = \mathbb{1}. \quad (12)$$

The relation spelled out in physical components states explicitly $W_{s_1} W'_{\chi(s_1, s_2, s_3)} W_{s_3} S = W_{s_1} S W_{s_2} W'_{s_3}$ for any combination of $s_1, s_2, s_3 \in \{0, 1\}$. Due to the mapping between \mathbf{W} and \mathbf{W}' , also the following dual relation holds,

$$P_{123} \mathbf{W}'_1 \mathbf{W}_2 \mathbf{W}'_3 S = \mathbf{W}'_1 S \mathbf{W}'_2 \mathbf{W}_3. \quad (13)$$

The equilibrium states can then be expressed in the following matrix product form,

$$\mathbf{p}^{(2n)} = \frac{1}{Z} \text{tr}(\mathbf{W}_1 \mathbf{W}'_2 \cdots \mathbf{W}'_{2n}), \quad \mathbf{p}'^{(2n)} = \frac{1}{Z} \text{tr}(\mathbf{W}'_1 \mathbf{W}_2 \cdots \mathbf{W}_{2n}), \quad (14)$$

with Z being fixed by the normalization. Using the relations (11) and (13) together with the properties $S^2 = \mathbb{1}$ and $P^2 = \mathbb{1}$, it is straightforward to see that the states $\mathbf{p}^{(2n)}$ and $\mathbf{p}'^{(2n)}$ are mapped to each other under the time propagation,

$$\mathbf{p}^{(2n)} = U_o \mathbf{p}'^{(2n)}, \quad \mathbf{p}'^{(2n)} = U_e \mathbf{p}^{(2n)}, \quad (15)$$

which implies their stationarity. Note that the exchange of the parameters $\xi \leftrightarrow \omega$ shifts the state in time for one step. Furthermore, the exchange of parameters also corresponds to the shift for one lattice site; explicitly

$$\eta(\mathbf{p}^{(2n)}) = \mathbf{p}'^{(2n)}, \quad \eta(\mathbf{p}'^{(2n)}) = \mathbf{p}^{(2n)}, \quad (16)$$

where η is the one-lattice-site shift operator, given in terms of a $2^{2n} \times 2^{2n}$ matrix $\eta_{(s_1 s_2 \dots s_{2n}), (b_1 b_2 \dots b_{2n})} = \delta_{s_2, b_1} \delta_{s_3, b_2} \delta_{s_4, b_3} \cdots \delta_{s_{2n}, b_{2n-1}} \delta_{s_1, b_{2n}}$. It can be argued that (14) provides a two parameter family of finitely correlated equilibrium states of the model, a kind of caricature of generalized Gibbs states.

2.4. Asymptotic equilibrium distributions of shorter configurations

The equilibrium distribution on a smaller subchain of length $2m$, $m \leq n$ can be expressed by summing over all the other sites

$$\mathbf{p}_{[1, 2m]}^{(2n)} = \frac{\text{tr}(\mathbf{W}_1 \mathbf{W}'_2 \mathbf{W}_3 \cdots \mathbf{W}'_{2m} T^{n-m})}{\text{tr} T^n}, \quad (17)$$

with the transfer matrix $T = (W_0 + W_1)(W'_0 + W'_1)$ taking the following form,

$$T = \begin{bmatrix} 1 + \xi\omega & \omega & \xi \\ 1 + \xi & \xi\omega & \xi \\ 1 + \omega & \omega & \xi\omega \end{bmatrix}. \quad (18)$$

Fixing the subchain length m while taking the thermodynamic limit $n \rightarrow \infty$ this reduces to

$$\mathbf{p}_{[1,2m]} = \lim_{n \rightarrow \infty} \mathbf{p}_{[1,2m]}^{(2n)} = \lambda^{-m} \frac{\langle l | \mathbf{W}_1 \mathbf{W}'_2 \mathbf{W}_3 \cdots \mathbf{W}'_{2m} | r \rangle}{\langle l | r \rangle}, \quad (19)$$

where λ is the leading eigenvalue of T ,

$$\lambda(\xi, \omega) = \frac{1}{3} \left(1 + 3\xi\omega + \left(\frac{\Delta}{2} \right)^{1/3} + (1 + 3\xi)(1 + 3\omega) \left(\frac{2}{\Delta} \right)^{1/3} \right), \quad (20)$$

$$\Delta = 2 + 9(\xi + \omega) + 27\xi\omega(2 + \xi + \omega) + \sqrt{27(\xi - \omega)^2(9\xi\omega(3\xi\omega - 2) - 4(\xi + \omega) - 1)},$$

and $\langle l |$, $|r\rangle$ are the corresponding left and right (unnormalized) eigenvectors,

$$\langle l | = \begin{bmatrix} (\lambda - \xi\omega)^2 - \xi\omega \\ \omega(\lambda - \xi\omega + \xi) \\ \xi(\lambda - \xi\omega + \omega) \end{bmatrix}^T, \quad |r\rangle = \begin{bmatrix} \omega(\lambda - \xi\omega + \xi) \\ (\lambda - \xi\omega)^2 - \lambda - \xi \\ \omega(\lambda - \xi\omega + \omega) \end{bmatrix}. \quad (21)$$

Note that the leading eigenvalue $\lambda(\xi, \omega)$ is the largest solution of the cubic equation

$$\lambda^3 - \lambda^2(1 + 3\xi\omega) - \lambda(\xi + \omega + \xi\omega(1 - 3\xi\omega)) - \xi\omega(1 - \xi\omega)^2 = 0, \quad (22)$$

that is larger than 1, and appears as a single (isolated) real root for all non-negative values of parameters ξ, ω .

The expression (19) holds for any finite subsection of the chain that starts at odd (even) sites at even (odd) times, i.e. the components of \mathbf{p} are probabilities of observing configurations $(s_x^t, s_{x+1}^t, \dots, s_{x+2m-1}^t)$ if $x + t \equiv 1 \pmod{2}$ holds. § In the other case, we have to exchange the role of parameters ξ and ω , i.e. $\mathbf{p}' = \mathbf{p}|_{\xi \leftrightarrow \omega}$. This can be summarized as

$$\begin{aligned} p \left(\begin{array}{cccc} \diamond & \diamond & \diamond & \diamond \\ s_1 & \cdots & \cdots & s_{2m} \\ \diamond & \diamond & \diamond & \diamond \end{array} \right) &:= p_{s_1 s_2 \dots s_{2m}} := \frac{\lambda^{-m}}{\langle l | r \rangle} \langle l | W_{s_1} W'_{s_2} \cdots W'_{s_{2m}} | r \rangle, \\ p \left(\begin{array}{cccc} \diamond & \diamond & \diamond & \diamond \\ s_2 & \cdots & \cdots & s_{2m} \\ \diamond & \diamond & \diamond & \diamond \end{array} \right) &:= p'_{s_1 s_2 \dots s_{2m}} := \frac{\lambda^{-m}}{\langle l' | r' \rangle} \langle l' | W'_{s_1} W_{s_2} \cdots W_{s_{2m}} | r' \rangle, \end{aligned} \quad (23)$$

where the new (primed) left/right vectors are obtained from the old (unprimed) ones by exchanging $\xi \leftrightarrow \omega$; $\langle l'(\xi, \omega) | = \langle l(\omega, \xi) |$ and $|r'(\xi, \omega)\rangle = |r(\omega, \xi)\rangle$.

The asymptotic equilibrium distribution on $2m$ sites (19) can be alternatively understood as a steady-state solution to a specific boundary driven chain, where the bulk dynamics is given by the deterministic update rules (4), while the boundary sites change stochastically (i.e. the situation studied in [10–13]). In Appendix A we provide the details about the equivalent stochastic boundary setup.

2.5. Statistical independence of solitons

The stationary (equilibrium) distributions (14) are characterized by the *statistical independence of solitons*, i.e. the probability of encountering a soliton is the same

§ Since $\mathbf{p}_{[1,2m]}$ is well defined for any m , the subscript will be omitted and the exact length specified when ambiguous. In what follows, \mathbf{p} will always refer to the asymptotic equilibrium distribution.

everywhere, independent of the positions of other solitons. This is a consequence of the fact that the conditional probability of observing (s_{2k-1}, s_{2k}) given the previous configuration $(s_1, s_2, \dots, s_{2k-2})$ depends only on the value of the last four bits, $(s_{2k-3}, s_{2k-2}, s_{2k-1}, s_{2k})$. Explicitly,

$$\frac{p_{s_1 s_2 \dots s_{2k-1} s_{2k}}}{p_{s_1 s_2 \dots s_{2k-2}}} = \frac{p_{s_{2k-3} s_{2k-2} s_{2k-1} s_{2k}}}{p_{s_{2k-3} s_{2k-2}}}, \quad \frac{p'_{s_1 s_2 \dots s_{2k-1} s_{2k}}}{p'_{s_1 s_2 \dots s_{2k-2}}} = \frac{p'_{s_{2k-3} s_{2k-2} s_{2k-1} s_{2k}}}{p'_{s_{2k-3} s_{2k-2}}}. \quad (24)$$

A similar relation holds for the conditional probability of finding (s_1, s_2) on the first two sites given that the sites from 3 to $2k$ are in the configuration $(s_3, s_4, \dots, s_{2k})$;

$$\frac{p_{s_1 s_2 \dots s_{2k}}}{p_{s_3 s_4 \dots s_{2k}}} = \frac{p_{s_1 s_2 s_3 s_4}}{p_{s_3 s_4}}, \quad \frac{p'_{s_1 s_2 \dots s_{2k}}}{p'_{s_3 s_4 \dots s_{2k}}} = \frac{p'_{s_1 s_2 s_3 s_4}}{p'_{s_3 s_4}}. \quad (25)$$

A proof of these relations simply follows from the sparse structure of the matrices W_s , W'_s , as is shown in Appendix B, and can be understood as the consequence of the so-called *patch-state ansatz* representation of the equilibrium state [10]. Intuitively, this implies that due to the *pure contact* (local) interactions between particles the equilibrium state can be interpreted as an ideal gas of solitons.

Taking into account (24) and (25) we can now introduce probabilities of observing left/right movers, p_l and p_r . The first parameter, p_l , is the conditional probability of observing a left mover, if we know that the neighbouring left ray does not contain a left moving soliton. This can be easily expressed in terms of equilibrium probabilities as follows,

$$p_l = \frac{p(\blacklozenge\blacklozenge) + p(\blacklozenge\blacktriangleright)}{p(\blacklozenge)} = \frac{p(\blacklozenge\blacklozenge) + p(\blacklozenge\blacktriangleright)}{p(\blacklozenge)} = \frac{\xi(\lambda + \omega(1 - \xi))}{\lambda(1 + \xi) + \xi(1 - \xi\omega)}. \quad (26)$$

Similarly, p_r is the conditional probability of observing a right moving soliton given that the neighbouring right ray does not contain a right mover,

$$p_r = \frac{p(\blacklozenge\blacklozenge) + p(\blacklozenge\blacktriangleleft)}{p(\blacklozenge)} = \frac{p(\blacklozenge\blacklozenge) + p(\blacklozenge\blacktriangleleft)}{p(\blacklozenge)} = \frac{\omega(\lambda + \xi(1 - \omega))}{\lambda(1 + \omega) + \omega(1 - \xi\omega)}. \quad (27)$$

Note that the shift for one time step or one lattice site maps p_r to p_l and vice versa; $p_l \xrightarrow{\xi \leftrightarrow \omega} p_r$.

3. Probability distributions of configurations in time

We now proceed to the main result of the paper, the construction of the matrix product representation of the *time state* \mathbf{q} . The components of the probability vector $q_{b_0 b_1 \dots b_{m-1}}$ are the probabilities of encountering multi-time configurations encoded by bit strings $(b_0, b_1, \dots, b_{m-1}) \in \{0, 1\}^m$ in the middle vertical saw, while the horizontal chain configurations (say along the bottom saw) are distributed according to the equilibrium state \mathbf{p} (schematically depicted in Fig. 1). Explicitly,

$$q_{b_0 b_1 \dots b_{m-1}} = \sum_{\underline{s} \equiv (s_{-m}, s_{-m+1}, \dots, s_{m-1})} p_{\underline{s}} \delta_{b_0, s_0^0} \delta_{b_1, s_1^1} \delta_{b_2, s_2^2} \delta_{b_3, s_3^3} \cdots \delta_{b_{m-1}, s_{\text{mod}(m-1, 2)}^{m-1}}, \quad (28)$$

s_k^t is the value at site k of the configuration $\underline{s} = (s_{-m}, s_{-m+1}, \dots, s_{m-1})$ propagated for t time steps starting from initial data $s_k^0 = s_k$. Due to the staggering, we should consider the site 0 at even time steps and the site 1 at odd time steps. The last site, whether 0 or 1, therefore depends on the parity of m . \parallel

Since the positions of the solitons in the equilibrium state \mathbf{p} are statistically independent, the probability of a left (right) mover reaching the central site at time t does not depend on the previously observed solitons, as long as there was no left (right) mover in the previous time step $t - 1$. Therefore, the conditional probability of observing a vertical configuration $(b_0, b_1, b_2, \dots, b_{k-1}, b_k)$ given the previous configuration $(b_0, b_1, b_2, \dots, b_{k-1})$ depends only on the last 4 bits, which implies a relation similar to (24) and (25),

$$\frac{q_{b_0 b_1 \dots b_{2k-1}}}{q_{b_0 b_1 \dots b_{2k-2}}} = f(b_{2k-4}, b_{2k-3}, b_{2k-2}, b_{2k-1}), \quad \frac{q_{b_0 b_1 \dots b_{2k}}}{q_{b_0 b_1 \dots b_{2k-1}}} = f'(b_{2k-3}, b_{2k-2}, b_{2k-1}, b_{2k}), \quad (29)$$

where we introduced two yet unknown functions of the last four bits, $f, f' : \mathbb{Z}_2 \times \mathbb{Z}_2 \times \mathbb{Z}_2 \times \mathbb{Z}_2 \rightarrow \mathbb{R}_{\geq 0}$, that have to be mapped into each other under the exchange of the spectral parameters ξ and ω (or equivalently, p_r and p_l),

$$f(b_1, b_2, b_3, b_4) \xleftrightarrow{p_l \leftrightarrow p_r} f'(b_1, b_2, b_3, b_4). \quad (30)$$

To determine the functions f, f' , one should first classify all the vertical configurations of 3 sites and their transitions into 4-site configurations. They can be divided into 3 different types.

- A configuration might be *inaccessible*, i.e. the configuration is inconsistent with the time evolution rules (4). The probability of obtaining such configurations is 0. These are the following,

$$\begin{array}{cccc} \begin{array}{c} \blacklozenge \\ \blacklozenge \\ \blacklozenge \end{array} & \begin{array}{c} \blacklozenge \\ \blacklozenge \\ \blacklozenge \end{array} & \begin{array}{c} \blacklozenge \\ \blacklozenge \\ \blacklozenge \end{array} & \begin{array}{c} \blacklozenge \\ \blacklozenge \\ \blacklozenge \end{array} \end{array} \quad (31)$$

- A configuration is allowed and the local update rules deterministically determine the next bit, i.e. the conditional probability $q_{b_{k-3} b_{k-2} b_{k-1} b_k} / q_{b_{k-3} b_{k-2} b_{k-1}}$ of observing b_k is either equal to 0 or 1. The following 3 configurations are of this type (probability 1),

$$\begin{array}{ccc} \begin{array}{c} \blacklozenge \\ \blacklozenge \\ \blacklozenge \end{array} \xrightarrow{1} \begin{array}{c} \blacklozenge \\ \blacklozenge \\ \blacklozenge \end{array} & \begin{array}{c} \blacklozenge \\ \blacklozenge \\ \blacklozenge \end{array} \xrightarrow{1} \begin{array}{c} \blacklozenge \\ \blacklozenge \\ \blacklozenge \end{array} & \begin{array}{c} \blacklozenge \\ \blacklozenge \\ \blacklozenge \end{array} \xrightarrow{1} \begin{array}{c} \blacklozenge \\ \blacklozenge \\ \blacklozenge \end{array} \end{array} \quad (32)$$

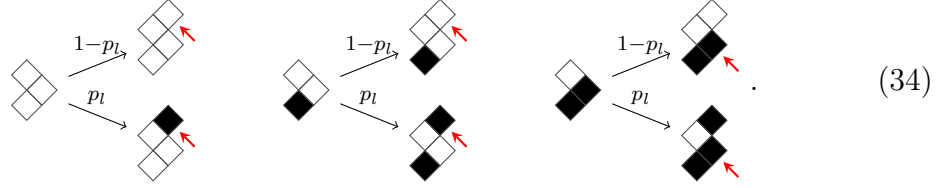
and analogously for the other parity of k (i.e. considering flipped configurations),

$$\begin{array}{ccc} \begin{array}{c} \blacklozenge \\ \blacklozenge \\ \blacklozenge \end{array} \xrightarrow{1} \begin{array}{c} \blacklozenge \\ \blacklozenge \\ \blacklozenge \end{array} & \begin{array}{c} \blacklozenge \\ \blacklozenge \\ \blacklozenge \end{array} \xrightarrow{1} \begin{array}{c} \blacklozenge \\ \blacklozenge \\ \blacklozenge \end{array} & \begin{array}{c} \blacklozenge \\ \blacklozenge \\ \blacklozenge \end{array} \xrightarrow{1} \begin{array}{c} \blacklozenge \\ \blacklozenge \\ \blacklozenge \end{array} \end{array} \quad (33)$$

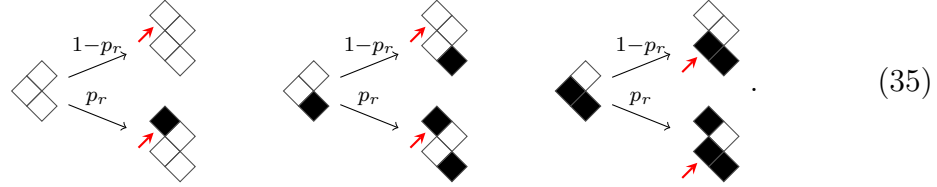
Complementary diagrams with negated b_k are associated with conditional probability 0.

\parallel Note also that the labels of the sites now go from $-m$ to $m - 1$ and no longer from 1 to $2m$. The convention is such that the sites with the even labels are getting propagated in the first half step and the sites with the odd labels in the second one, no matter the parity of m .

- A configuration is allowed and both the configurations $(b_{k-3}b_{k-2}b_{k-1}0)$ and $(b_{k-3}b_{k-2}b_{k-1}1)$ are also allowed. These are the following,



The conditional probabilities $q_{b_{k-3}b_{k-2}b_{k-1}b_k}/q_{b_{k-3}b_{k-2}b_{k-1}}$ correspond to the probability of a left mover (not)reaching the vertical saw (corresponding to the top/bottom option respectively) at the position indicated by the red arrows. Since the solitons in the equilibrium state are independent, the probability p_l is given by (26). For the flipped configurations, everything works similarly, only p_l has to be replaced by p_r from (27),



Extracting the precise values of $f(b_1, b_2, b_3, b_4)$ and $f'(b_1, b_2, b_3, b_4)$ from the diagrams (31–35), the probability of a vertical configuration can be explicitly expressed as a patch state

$$q_{b_0b_1\dots b_k} = q_{b_0b_1b_2}f(b_0, b_1, b_2, b_3)f'(b_1, b_2, b_3, b_4)\cdots f^{(\prime)}(b_{k-3}, b_{k-2}, b_{k-1}, b_k), \quad (36)$$

where the last term is $f(b_{k-3}, b_{k-2}, b_{k-1}, b_k)$ if k is odd and $f'(b_{k-3}, b_{k-2}, b_{k-1}, b_k)$ otherwise. The values of the probabilities of the configurations of length 3 can be determined by requiring $\sum_{b_0, b_1} q_{b_0b_1b_2b_3b_4} = q_{b_2b_3b_4}$.

The probability vector (36) can be efficiently encoded with an MPA form by introducing a 3 dimensional auxiliary space, with the basis vectors $|0\rangle, |1\rangle, |2\rangle$ keeping the relevant information about the last three bits. The pairs of matrices $A_s(p_r, p_l)$, $A'_s(p_r, p_l)$ and left/right boundary vectors $(L(p_r, p_l)|, |R(p_r, p_l))$ are constructed so that the probability vector \mathbf{q} is expressed as

$$\mathbf{q} = (L|\mathbf{A}_0\mathbf{A}'_1\mathbf{A}_2\cdots\mathbf{A}_k^{(\prime)}|R). \quad (37)$$

The last matrix is either \mathbf{A} or \mathbf{A}' , depending on the parity of the last index k . The matrices $A_s(p_r, p_l)$, contain the relevant transition rates f, f' ,

$$A_0 = \begin{bmatrix} 1-p_r & 0 & 0 \\ 0 & 0 & 0 \\ 1 & 0 & 0 \end{bmatrix}, \quad A_1 = \begin{bmatrix} 0 & p_r & 0 \\ 0 & 0 & 1 \\ 0 & 0 & 0 \end{bmatrix}, \quad (38)$$

and the other pair of matrices is obtained by replacing p_r with p_l ,

$$\mathbf{A}'(p_r, p_l) = \mathbf{A}(p_l, p_r). \quad (39)$$

The left and right vectors $\langle L|$, $|R\rangle$ are the left and right eigenvector of the matrix $\mathcal{T} = (A_0 + A_1)(A'_0 + A'_1)$ that correspond to the leading eigenvalue (which is 1), namely,

$$\langle L| = \frac{1}{1 + p_r + p_l} \begin{bmatrix} 1 & p_l & p_r \end{bmatrix}, \quad |R\rangle = \begin{bmatrix} 1 \\ 1 \\ 1 \end{bmatrix}. \quad (40)$$

Additionally, this choice of $|R\rangle$ works for both parities of k , since $|R\rangle$ is an eigenvector corresponding to the eigenvalue 1 of both $A_0 + A_1$ and $A'_0 + A'_1$. The normalization of the boundary vectors is determined by the normalization condition of the probability vector \mathbf{q} ,

$$\sum_{b_0, b_1, b_2, \dots, b_k} q_{b_0 b_1 b_2 \dots b_k} = \langle L| \overbrace{(A_0 + A_1)(A'_0 + A'_1)(A_0 + A_1) \cdots}^{k+1} |R\rangle = \langle L|R\rangle = 1. \quad (41)$$

4. 2-point correlation functions

Since the matrices \mathbf{A} , \mathbf{A}' are finitely dimensional, many physically interesting quantities can now be expressed explicitly. The simplest example is the 2-point density-density correlation function at different times and the same position,

$$C(t) = \langle \rho(0, 0)\rho(0, t) \rangle - \langle \rho(0, 0) \rangle^2, \quad (42)$$

where $\rho(x, t)$ is the density at position x and time t and $\langle \cdot \rangle$ is the expectation value with respect to the (horizontal) stationary state. The correlation function is the $x = 0$ part of the spatio-temporal correlation function computed in [14], but here the underlying equilibrium state is richer and not limited to the maximum entropy (*infinite temperature*) state considered in Ref. [14].

For simplicity, let us consider even times $t = 2m$. Then the correlation function takes the following matrix product form,

$$\begin{aligned} C(2m) &= \langle L| A_1 \overbrace{(A'_0 + A'_1)(A_0 + A_1) \cdots (A'_0 + A'_1)}^{2m-1} A_1 |R\rangle - \langle L| A_1 |R\rangle^2 \\ &= \langle L| A_1 (A'_0 + A'_1) \mathcal{T}^{m-1} A_1 |R\rangle - \frac{(p_l + p_r)^2}{(1 + p_l + p_r)^2}, \end{aligned} \quad (43)$$

where \mathcal{T} is a *temporal transfer matrix*, i.e. the product of sums of both types of MPA matrices, $\mathcal{T} = (A_0 + A_1)(A'_0 + A'_1)$, as introduced earlier. The correlation function decays exponentially with the exact form given by

$$C(2m) = \frac{(\Lambda_2^m - \Lambda_3^m)((p_l + p_r)^2 - p_l p_r (1 + p_l + p_r)) + (\Lambda_2^{m-1} - \Lambda_3^{m-1}) p_l p_r (p_l + p_r)}{(1 + p_l + p_r)^2 (\Lambda_3 - \Lambda_2)}, \quad (44)$$

where $\Lambda_{2,3}$ are the subleading eigenvalues of the matrix \mathcal{T} , ¶

$$\Lambda_{2,3} = -\frac{1}{2} \left(p_l + p_r - p_l p_r \pm \sqrt{(p_l + p_r - p_l p_r)^2 - 4p_l p_r} \right). \quad (45)$$

¶ Note that this holds only for $\Lambda_2 \neq \Lambda_3$. If the subleading eigenvalues are degenerate the exact form of the correlation function is slightly changed, but asymptotically the decay is still exponential.

In the maximum entropy state, i.e. $\xi = \omega = 1$ or $p_l = p_r = \frac{1}{2}$, the correlation function can be recast as

$$C^\infty(2m) = 2^{-3m-4} \left(\left(-1 - \frac{i}{\sqrt{7}} \right) \left(-3 - i\sqrt{7} \right)^m + \left(-1 + \frac{i}{\sqrt{7}} \right) \left(-3 + i\sqrt{7} \right)^m \right), \quad (46)$$

which agrees with the result of [14].

5. Probabilities of time-configurations and the absence of decoupling of timescales in RCA54

Even though the 2-point correlation function is a generalization of the previous result [14], the true advantage of the time MPA is the ability to easily express multi-point correlation functions of observables at one specific location in space (such as the origin). An extreme case are the probabilities of time configurations themselves. These can be alternatively recast in an equivalent (non MPA) form as,

$$q_{s_1, s_2, \dots, s_k} = \delta_{n_1, 0} \frac{(1 - p_l)^{n_2} (1 - p_r)^{n_3} p_r^{n_4} p_l^{n_5}}{1 + p_l + p_r}, \quad (47)$$

with $\{n_j, j = 1, \dots, 5\}$ being a set of integer indicators that characterize the number of left and right movers in the configuration (s_1, s_2, \dots, s_k) ,

$$\begin{aligned} n_1 &= \sum_{j=2}^{k-1} s_j (1 - (s_{j-1} - s_{j+1})^2), & n_2 &= \sum_{j=1}^{\lfloor k/2 \rfloor} (1 - s_{2j-1})(1 - s_{2j}), \\ n_3 &= \sum_{j=1}^{\lfloor (k-1)/2 \rfloor} (1 - s_{2j})(1 - s_{2j+1}), & n_4 &= \sum_{j=1}^{\lfloor k/2 \rfloor} s_{2j-1} s_{2j} + \text{mod}(k+1, 2)(1 - s_{k-1})s_k, \\ n_5 &= s_1(1 - s_2) + \sum_{j=1}^{\lfloor (k-1)/2 \rfloor} s_{2j} s_{2j+1} + \text{mod}(k, 2)(1 - s_{k-1})s_k. \end{aligned} \quad (48)$$

The expression (47) is equivalent to the appropriate component of the time vector (37), which can be straightforwardly checked.

The result above gives access to the full distribution of timescales associated with the dynamics of a single site, when tracing out the rest of the system. This is particularly important information in systems that display complex dynamics and are therefore likely to exhibit non-trivial distributions of local times. As a particular example we consider the distributions of *exchange* and *persistence* times in the RCA54. The definitions are those used in the literature on supercooled liquids, see [16, 17]. The exchange time is the time between two events, for example a spin flip, after a previous event has occurred. The persistence time is the time to the next event starting from an arbitrary time, i.e. not conditioned on the previous event having occurred at the start of the time segment under consideration.

If the statistics of events is *Poissonian*, persistence and exchange times are equally (and exponentially) distributed. However, when there are non-trivial correlations between events, both types of times measure different properties of the underlying

process and their distributions differ. For example, in stochastic kinetically constrained models (KCMs) of glasses, such as the Fredrickson-Andersen (FA) or the East model [18–20], the two timescales behave very differently, with the average persistence time growing much faster with decreasing temperature than the average exchange time, a phenomenon known as *transport decoupling* [16, 17]. The reason is that the dynamics of these stochastic KCMs is intermittent, and when projected to a single site it leads to bunching of flip events on the site. In this case the exchange time is dominated by the bunched events, while the persistence time is dominated by the long stretches between bunches. It is interesting to consider the possibility of timescale decoupling in the RCA54 as the dynamical rule (2) imposes a constraint that is similar to that of the FA model (flips can only occur if at least one nearest neighbour is excited). Furthermore, the RCA54 displays dynamical large deviation transitions [13] similar to those of the FA model [21], which indicates the presence of non-trivial fluctuations in the trajectories of the dynamics.

For the RCA54 we define the exchange time as the time between two consecutive observed particles (excitations) in a time configuration, and define the persistence time as a time before the next particle if we start observing the state at some point without a particle. The probability of observing an exchange time equal to t , $p_E(t)$, can be simply expressed in terms of probabilities of time configurations of the form $100\dots 01$,

$$p_E(t) \propto \frac{1}{2} \left(\underbrace{q_{100\dots 01}}_t + \underbrace{q_{0100\dots 01}}_t + \underbrace{q_{1100\dots 01}}_t \right), \quad \sum_{t=1}^{\infty} p_E(t) = 1, \quad (49)$$

where we average over the even/odd starting positions of the time configuration. Note that the second term can be dropped since subsequence 010 is forbidden. Similarly, the probability of persistence time being equal to t , $p_P(t)$, is up to normalization equal to

$$p_P(t) \propto \frac{1}{2} \left(\underbrace{q_{00\dots 01}}_t + \underbrace{q_{000\dots 01}}_t + \underbrace{q_{100\dots 01}}_t \right), \quad \sum_{t=1}^{\infty} p_P(t) = 1. \quad (50)$$

The two distributions are related by

$$p_P(t) - p_P(t+1) = \frac{p_E(t)}{\langle t_E \rangle}, \quad (51)$$

which is the discrete time version of the usual relation between persistence and exchange distributions in continuous time dynamics. Here, $\langle t_{E/P} \rangle$ are mean exchange and persistence times, $\langle t_{E/P} \rangle = \sum_{t=1}^{\infty} t p_{E/P}(t)$.

Using the simplified expressions for probabilities (47) it is easy to see that the exchange and persistence time distributions reduce to the following form,

$$p_E(t) = \begin{cases} \frac{p_l^2(1-p_r)+p_r^2(1-p_l)}{p_l+p_r} ((1-p_l)(1-p_r))^{t/2-1}, & t \equiv 0 \pmod{2}, \\ \frac{2p_l p_r}{p_l+p_r} ((1-p_l)(1-p_r))^{(t-1)/2}, & t \equiv 1 \pmod{2}, \end{cases} \quad (52)$$

$$p_P(t) = \begin{cases} \frac{p_l(1-p_r)+p_r(1-p_l)}{2} ((1-p_l)(1-p_r))^{t/2-1}, & t \equiv 0 \pmod{2}, \\ \frac{p_l+p_r}{2} ((1-p_l)(1-p_r))^{(t-1)/2}, & t \equiv 1 \pmod{2}. \end{cases}$$

If the parameters p_l, p_r coincide, the two distributions are the same. Otherwise they differ, but the deviations from the Poissonian statistics are small and can be understood as a consequence of short-range correlations of the time state. Specifically, computing the average exchange and persistence times,

$$\langle t_E \rangle = \frac{2}{p_l + p_r}, \quad \langle t_P \rangle = \frac{4 - p_l - p_r}{2(p_l + p_r - p_l p_r)}, \quad (53)$$

we observe that their ratio is bounded from top and bellow as

$$1 \geq \frac{\langle t_P \rangle}{\langle t_E \rangle} \geq \frac{3}{4}, \quad (54)$$

which indicates that overall the two timescales scale similarly with the parameters that control the dynamics, in contrast to what occurs in the FA model [16,17] where the ratio of $\langle t_P \rangle$ to $\langle t_E \rangle$ is larger than one and increases with decreasing temperature (or equivalent parameters that control the speed of relaxation). This also means that unlike stochastic KCMs, to quantify non-trivial correlations in the dynamics of the RCA54 (cf. [13]), it is necessary to consider multi-point correlators both in time and space (not just in time as above).

6. Conclusion

We have constructed an explicit matrix product form of the time state \mathbf{q} in the case of Rule 54 reversible cellular automaton. The construction was possible due to the simple structure of the equilibrium state \mathbf{p} , which contains left and right movers that are statistically independent, as long as they follow an exclusion rule. The MPA form of the vector \mathbf{q} allows us to efficiently express correlation functions and expectation values of time configurations, i.e. multi-time correlation functions. For instance, we have computed 2-point correlation function and shown that in the limit $\xi = \omega = 1$ (i.e. in the maximum entropy state) it agrees with the result of Ref [14]. Furthermore, it is possible to express the probabilities of time configurations in terms of numbers of left and right movers, which enabled us to exactly express the distributions of exchange and persistence times and show the absence of timescale decoupling in the model.

The work presented in the paper opens some new research questions. The first one is the generalization of the result to other time-translation invariant (equilibrium) states. The model exhibits an infinite number of conserved quantities, therefore it is possible to construct stationary states \mathbf{p} that are characterized by more than 2 free parameters. The question is if it is still possible to obtain an efficient MPA representation of the time state and what is the dimensionality of the necessary auxiliary space.

Even though the construction of time state is straightforward, one would like to obtain some algebraic interpretation by e.g. finding relations similar to the cubic algebra in [12,13]. They could provide simpler means of extracting physically interesting quantities, as well as contribute additional insight into the integrability structure of the model.

Most prominently, one would like to apply the concept to other lattice dynamical systems. This is intimately connected to the previous question of understanding the solution from an algebraic point of view, which is more robust and does not rely on particularities of the model and the underlying stationary state. Preliminary empirical results suggest that generically, the computational complexity of the time state grows exponentially with time, however one could hope to devise an approximate numerical scheme to efficiently simulate the dynamics (time state) at $x = 0$ using MPA as a variational ansatz [22].

Acknowledgments

This work has been supported by the European Research Council under the Advanced Grant No. 694544 - OMNES, by the Slovenian Research Agency (ARRS) under the Programme P1-0402, and by the Leverhulme Trust Grant No. RPG-2018-181.

References

- [1] Chandler D and Garrahan J P 2010 *Annu. Rev. Phys. Chem.* **61** 191–217 <http://dx.doi.org/10.1146/annurev.physchem.040808.090405>
- [2] Binder K and Kob W 2011 *Glassy materials and disordered solids: An introduction to their statistical mechanics* (Singapore: World Scientific)
- [3] Biroli G and Garrahan J P 2013 *J. Chem. Phys.* **138** 12A301 <http://link.aip.org/link/?JCP/138/12A301/1>
- [4] Spohn H 2014 *J. Stat. Phys.* **154** 1191–1227 <https://link.springer.com/article/10.1007/s10955-014-0933-y>
- [5] Bobenko A, Bordemann M, Gunn C and Pinkall U 1993 *Commun. Math. Phys.* **158** 127–134 <https://doi.org/10.1007/BF02097234>
- [6] Takesue S 1987 *Phys. Rev. Lett.* **59**(22) 2499–2502 <https://link.aps.org/doi/10.1103/PhysRevLett.59.2499>
- [7] Gopalakrishnan S 2018 *Phys. Rev. B* **98**(6) 060302 <https://link.aps.org/doi/10.1103/PhysRevB.98.060302>
- [8] Gopalakrishnan S, Huse D A, Khemani V and Vasseur R 2018 *Phys. Rev. B* **98**(22) 220303 <https://link.aps.org/doi/10.1103/PhysRevB.98.220303>
- [9] Friedman A J, Gopalakrishnan S and Vasseur R 2019 *arXiv:1905.03265* <https://arxiv.org/abs/1905.03265>
- [10] Prosen T and Mejía-Monasterio C 2016 *J. Phys. A: Math. Theor.* **49** 185003 <http://stacks.iop.org/1751-8121/49/i=18/a=185003>
- [11] Inoue A and Takesue S 2018 *J. Phys. A: Math. Theor.* **51** 425001 <https://doi.org/10.1088/1751-8121/51/18/425001>
- [12] Prosen T and Buča B 2017 *J. Phys. A: Math. Theor.* **50** 395002 <http://stacks.iop.org/1751-8121/50/i=39/a=395002>
- [13] Buča B, Garrahan J P, Prosen T and Vanicat M 2019 *Phys. Rev. E* **100**(2) 020103 <https://link.aps.org/doi/10.1103/PhysRevE.100.020103>
- [14] Klobas K, Medenjak M, Prosen T and Vanicat M 2019 *Commun. Math. Phys.* <https://doi.org/10.1007/s00220-019-03494-5>
- [15] Alba V, Dubail J and Medenjak M 2019 *Phys. Rev. Lett.* **122**(25) 250603 <https://link.aps.org/doi/10.1103/PhysRevLett.122.250603>
- [16] Jung Y, Garrahan J and Chandler D 2004 *Phys. Rev. E* **69** <http://dx.doi.org/10.1103/PhysRevE.69.061205>

- [17] Jung Y, Garrahan J P and Chandler D 2005 *J. Chem. Phys.* **123** 084509 <https://aip.scitation.org/doi/abs/10.1063/1.2001629>
- [18] Fredrickson G H and Andersen H C 1984 *Phys. Rev. Lett.* **53** 1244–1247 <https://link.aps.org/doi/10.1103/PhysRevLett.53.1244>
- [19] Jäckle J and Eisinger S 1991 *Z. fur Phys. B* **84** 115–124 ISSN 0722-3277 <http://dx.doi.org/10.1007/BF01453764>
- [20] Garrahan J P 2018 *Physica A* **504** 130–154 <https://doi.org/10.1016/j.physa.2017.12.149>
- [21] Garrahan J P, Jack R L, Lecomte V, Pitard E, van Duijvendijk K and van Wijland F 2007 *Phys. Rev. Lett.* **98**(19) 195702 <http://dx.doi.org/10.1103/PhysRevLett.98.195702>
- [22] Schollwöck U 2011 *Ann. Phys.* **326** 96–192 <https://doi.org/10.1016/j.aop.2010.09.012>

Appendix A. Boundary driving with the steady state that corresponds to the asymptotic probability distribution on a finite chain

We would like to connect the MPA form of the vectors \mathbf{p} , \mathbf{p}' , introduced in (23), with an equivalent MPA solution of a boundary driven setup. This amounts to constructing boundary two-site propagators, $P^{L/R}$, so that $U_{e/o}$, defined as

$$U_e = P_{123}P_{345} \cdots P_{2m-3\ 2m-2\ 2m-1} P_{2m-1\ 2m}^R, \quad U_o = P_{12}^L P_{234} P_{456} \cdots P_{2m-2\ 2m-1\ 2m}, \quad (\text{A.1})$$

map \mathbf{p} to \mathbf{p}' and vice versa.

Taking into account the bulk relations (11) and (13), it suffices that the following boundary equations are satisfied,

$$\begin{aligned} \langle l | \mathbf{W}_1 S = \alpha \langle l' | \mathbf{W}'_1, & \quad P_{12}^L (\langle l' | \mathbf{W}'_1 \mathbf{W}_2 S) = \gamma \langle l | \mathbf{W}_1 \mathbf{W}'_2, \\ \mathbf{W}'_{2m} S | r' \rangle = \delta \mathbf{W}'_{2m} | r \rangle, & \quad P_{2m-1\ 2m}^R (\mathbf{W}'_{2m-1} S \mathbf{W}'_{2m} | r \rangle) = \beta \mathbf{W}'_{2m-1} \mathbf{W}_{2m} | r' \rangle, \end{aligned} \quad (\text{A.2})$$

where the parameters α , β , γ and δ have to fulfill the following condition

$$\alpha\beta = \frac{\langle l|r \rangle}{\langle l'|r' \rangle} = \frac{1}{\gamma\delta}. \quad (\text{A.3})$$

Solving these equations, we obtain the following boundary propagators,

$$P^R = \begin{bmatrix} 1 - p_l & 1 - p_l & 0 & 0 \\ p_l & p_l & 0 & 0 \\ 0 & 0 & 0 & 1 \\ 0 & 0 & 1 & 0 \end{bmatrix}, \quad P^L = \begin{bmatrix} 1 - p_r & 0 & 1 - p_r & 0 \\ 0 & 0 & 0 & 1 \\ p_r & 0 & p_r & 0 \\ 0 & 1 & 0 & 0 \end{bmatrix}, \quad (\text{A.4})$$

with the parameters p_r , p_l corresponding to the conditional probabilities of observing right/left movers as expressed in (27), (26), and the following values of α , β , γ , δ ,

$$\begin{aligned} \alpha &= \frac{\lambda + \xi - \xi\omega}{\lambda + \omega - \xi\omega}, & \beta &= \frac{\omega}{\xi}, \\ \gamma &= 1, & \delta &= \frac{\xi(\lambda + \omega - \xi\omega)}{\omega(\lambda + \xi - \xi\omega)}. \end{aligned} \quad (\text{A.5})$$

Note that the choice of $P^{R,L}$ is not unique and this is only one possible form.

The boundary relations (A.2) and the solution (23) are simpler than the ones considered in [12], since the boundary vectors do not depend on the configuration of the boundary sites. These states therefore represent a specific subset of solutions found in the previous works [10–12].

Appendix B. Conditional probabilities of observing subconfigurations

To prove the relations (24) and (25), we observe that the vectors $\langle l | W_{s_1} W'_{s_2} W_{s_3} W'_{s_4}$ and $\langle l | W_{s_3} W'_{s_4}$ (similarly $W_{s_1} W'_{s_2} W_{s_3} W'_{s_4} | r \rangle$ and $W_{s_1} W'_{s_2} | r \rangle$) are linearly dependent. Explicitly, for every 4-site configuration (s_1, s_2, s_3, s_4) there exist scalar factors $c_{s_1 s_2 s_3 s_4}^{(l)}$ and $c_{s_1 s_2 s_3 s_4}^{(r)}$, so that the following holds,

$$\langle l | W_{s_1} W'_{s_2} W_{s_3} W'_{s_4} = c_{s_1 s_2 s_3 s_4}^{(l)} \langle l | W_{s_3} W'_{s_4}, \quad (\text{B.1})$$

$$W_{s_1} W'_{s_2} W_{s_3} W'_{s_4} | r \rangle = c_{s_1 s_2 s_3 s_4}^{(r)} W_{s_1} W'_{s_2} | r \rangle, \quad (\text{B.2})$$

which can be straightforwardly verified by checking all the 16 configurations. From here the relations (24) and (25) follow directly since for every even configuration length $2k$ the left-hand side of the first part of equation (24) can be rewritten as

$$\begin{aligned} & \frac{\langle l | W_{s_1} W'_{s_2} \cdots W_{s_{2k-3}} W'_{s_{2k-2}} W_{s_{2k-1}} W'_{s_{2k}} | r \rangle}{\langle l | W_{s_1} W'_{s_2} \cdots W_{s_{2k-3}} W'_{s_{2k-2}} | r \rangle} \\ &= \frac{c_{s_1 s_2 s_3 s_4}^{(l)} \cdots c_{s_{2k-5} s_{2k-4} s_{2k-3} s_{2k-2}}^{(l)} \langle l | W_{s_{2k-3}} W'_{s_{2k-2}} W_{s_{2k-1}} W'_{s_{2k}} | r \rangle}{c_{s_1 s_2 s_3 s_4}^{(l)} \cdots c_{s_{2k-5} s_{2k-4} s_{2k-3} s_{2k-2}}^{(l)} \langle l | W_{s_{2k-3}} W'_{s_{2k-2}} | r \rangle} \\ &= \frac{\langle l | W_{s_{2k-3}} W'_{s_{2k-2}} W_{s_{2k-1}} W'_{s_{2k}} | r \rangle}{\langle l | W_{s_{2k-3}} W'_{s_{2k-2}} | r \rangle}, \end{aligned} \quad (\text{B.3})$$

where the first equality follows from repeatedly applying the relation (B.1). From Eq. (B.2) we analogously obtain the following,

$$\frac{\langle l | W_{s_1} W'_{s_2} W_{s_3} W'_{s_4} \cdots W_{s_{2k-1}} W'_{s_{2k}} | r \rangle}{\langle l | W_{s_3} W'_{s_4} \cdots W_{s_{2k-1}} W'_{s_{2k}} | r \rangle} = \frac{\langle l | W_{s_1} W'_{s_2} W_{s_3} W'_{s_4} | r \rangle}{\langle l | W_{s_3} W'_{s_4} | r \rangle}. \quad (\text{B.4})$$

Note that the pair of relations dealing with the probabilities $p'_{\underline{s}}$ follows trivially after the exchange $\xi \leftrightarrow \omega$.